Solar Powered Unmanned Aerial Vehicle with Active Output Filter under Non-Linear Load Conditions

D.G.Himpalnerkar

Guided By
Dr.S.M.Shinde

Abstract: In this project,a new solar-powered unmanned aerial vehicle's electric powertrain (UAV) is proposed. The proposed system structure is based on the creation of a power supply system for both the Solong and Zyphyr aircraft models. The proposed UAV model incorporates the Zyphry UAV's use of an AC line feeder to power the propellers rather than DC power lines. Solar panels, an energy management system based on a lithium sulphide battery, an inverter, an AC bus-line, and an active output filter are all part of the proposed powertrain (AOF).The AOF topology is made up of a high switching frequency H-bridge inverter and a small LC filter. By incorporating an emulated series resistance with the H-bridge stage to ensure high quality pure sinusoidal waveform of the line voltage, the AOF system reduces the size and weight of the power transmission system while significantly improving its conversion efficiency.This emulated series resistance produces an injected voltage across it to diminish unwanted harmonics created from the non-linear load. A simulation model setup is created to simulate the proposed system and the system is tested under non-linear load condition with closed-loop feed-back control strategy. The obtained simulation and experimental results demonstrate that high-quality sinusoidal line voltage waveforms can be obtained using the active resistance compensation technique with total harmonic distortion factor less than 3%.

Keywords: Active output filter, active resistance compensation, loss analysis, non-linear load, solar powered, unmanned aerial vehicle.

INTRODUCTION: The main goal of using an electric powertrain system operating at a frequency of 400 Hz in aerospace applications instead of conventional low frequency of 50/60 Hz is to reduce the size and weight of the power transmission system [1]. Since conventional passive filters are one of the heaviest elements in power transmission systems due to their lower power intensity compared to the active power components. Therefore, reducing the size and weight of these filters will greatly reduce the size of the power system and thus reduce fuel

consumption [2]. The development of the aircraft electric powertrain systems has evolved over the years, passing through many stages until achieving fully developed unmanned aerial vehicle (UAV) technology. The mechanical based speed drives such as constant speed drives (CSD) and integrated engine generator (IDG) is developed to provide mechanical interface with the 400 Hz synchronous alternator [3]–[7]. The mechanical coupling is essentially a variable ratio hydro-mechanical drive that coupled the jet engine shaft to the synchronous alternator through multiple gear stages and hydraulic cylinder block common to both the pump and the motor. However, these mechanical interfaces have numerous disadvantages such as low efficiency, it requires frequent and costly maintenance, large size and weight [8], [9]. Towards more electric aircraft (MEA), the electrical systems have replaced tradition mechanical systems in modern aircrafts because of their excellent advantages in energy density, high conversion efficiency and requires less maintenance [20]. Therefore, a variable frequency drive (VFD) system has been introduced to eliminate the mechanical interface [10], [11]. However, this involves operating electrical loads over a frequency range. A significant enhancement in both powertrain system size and performance is achieved using variable speed constant frequency (VSCF) powertrain system [12]–[15]. The VSCF powertrain system comprises of a rectifier, a DC-link followed by a PWM inverter with passive (L-C) output filters to generate a sinusoidal load output voltage. The PWM inverter produces the required sinusoidal load voltage at constant frequency. However, VSCF also still has some weaknesses such the limiting switching frequency of PWM inverter in high power applications. Restrictions in the inverter switching frequency leads to a larger size of the elements of the LC output filter with a higher output impedance [16]. The realization of active filters to simulate passive filter components has allowed size reduction for many applications such as realizing passive inductance [17] and an active DC-link for adjustable speed drive systems [18]. It also improves system performance under non-linear load conditions [19]. The persistent progress in the aviation powertrain systems has resulted in a remotely piloted UAV that has been used in a wide range of increasing applications like communications, surveillance, investigations, weather broadcasting, and conducting military operations [21], [22]. However, UAV experiences from numerous difficulties, its continuous need for fossil fuel while flying to supply the combustion engine for aircraft propulsion and low flight endurance, short flight time and low flight endurance [23]. Thus, solar powered UAV has received substantial extent of attention from researchers. A solar-powered UAV utilizes solar energy as a substitute of

conventional fossil fuels, converting harvested solar energy into electrical energy to power an electric-propulsion system and other involved apparatus [24]–[27]. The DC-link propulsion system and energy management of the conventional solar powered UAV illustrated in Fig. 1(a) requires an energy storage system such as batteries for night flying or other low solar intensity times. Helios HP01 UAV, proposed by NASA, uses PV panels integrated with lithium ion-based battery pack system to supply 21kW loads of DC propellers [28]. Due to the heavy construction of lithium-ion battery, NASA proposed HELIOS HP03 model that uses hybrid PV and fuel cell power system. This topology has higher energy density and less energy loss compared to the conventional PV battery system. Regrettably, the Helios HP03 crashed after a 30-minute flight, and one of the main causes of this accident was the limited airframe caused by the fuel cell system. In 2005, Solong invented a novel AC drive system which provides a low DC-bus voltage [29]. The effective and lightweight of Solong design enabled it to break its first 48 straight hours of flight record. Subsequently, Zyphyr established PV with a high-power lithium-sulfur battery pack which still maintains the longest aviation endurance record [21] The inverter in the UAV power system is a crucial part because it handles full power, so any enhancement in the size and efficiency of the inverter will be significantly reflected in the aircraft [10], [20], [25]. Increasing the switching frequency in a PWM classic inverter results in high switching power loss. Conversely, reducing the switching frequency requires bulky passive LC output filters to provide a sinusoidal load output voltage [24]. Challenges to use the active filtration techniques by voltage or current injection have been made since the 1970's to reduce the use of passive filters [30]. In particular, series active filters are capable to suppress voltage harmonics generated by the load or source especially with aggressive deployment in inverter system into electrical vehicles with renewable energy systems [31]–[33]. However, they incorporate large coupling transformer design, and they are weaker in dealing with current harmonics caused by a non-linear load. Fig. 1 shows the development of the power generation system of solar powered UAV. The conventional solar powered UAV with constant DC-bus line to supply the propellers is illustrated in Fig. 1(a). AC-bus line using constant frequency PWM inverter with standard bulky passive L-C filter as a replacement of DC-bus line is shown in Fig. 1(b). Recently, active output filter (AOF) have been proposed for variable speed constant frequency aircraft system with six-step inverter to eliminate the need of coupling transformer, increasing the conversion efficiency and reduce the overall passive elements sizing in aerospace application [34], [35].

However, only linear loads are considered in these studies. This paper introduces a new electric powertrain system based on the concept of AOF for solar powered UAV to employ an effective filtration system instead of the use of traditional passive filters. This allows the main inverter that operates at the total rated power to operate at low switching frequency, thus, improves the overall efficiency of the powertrain system. The proposed architecture is a potential improvement to the power supply of both Solong and Zyphyr aircraft models. The proposed UAV model incorporates the Zyphry UAV use of an AC-bus line instead of DC-bus line to power electric motors and loads. The system also includes solar panels and an energy management system based on lithium sulfide batteries, inverter and AOF. The AOF consists of three individual H-bride inverters operating at high frequency and a compact LC power filter. The AOF system is operated at fraction of the rated power of the electrical system, therefore, reduces the size of the power transmission system and significantly improves its conversion efficiency. The system is simulated and tested under non-linear loads using a closed loop control strategy. Active compensation technology is employed to ensure high quality of sinusoidal voltage waveforms at the terminals of the non-linear load. A simulation model is created in Matlab Simulink to simulate the proposed system, and the obtained results proved the efficiency of the system.

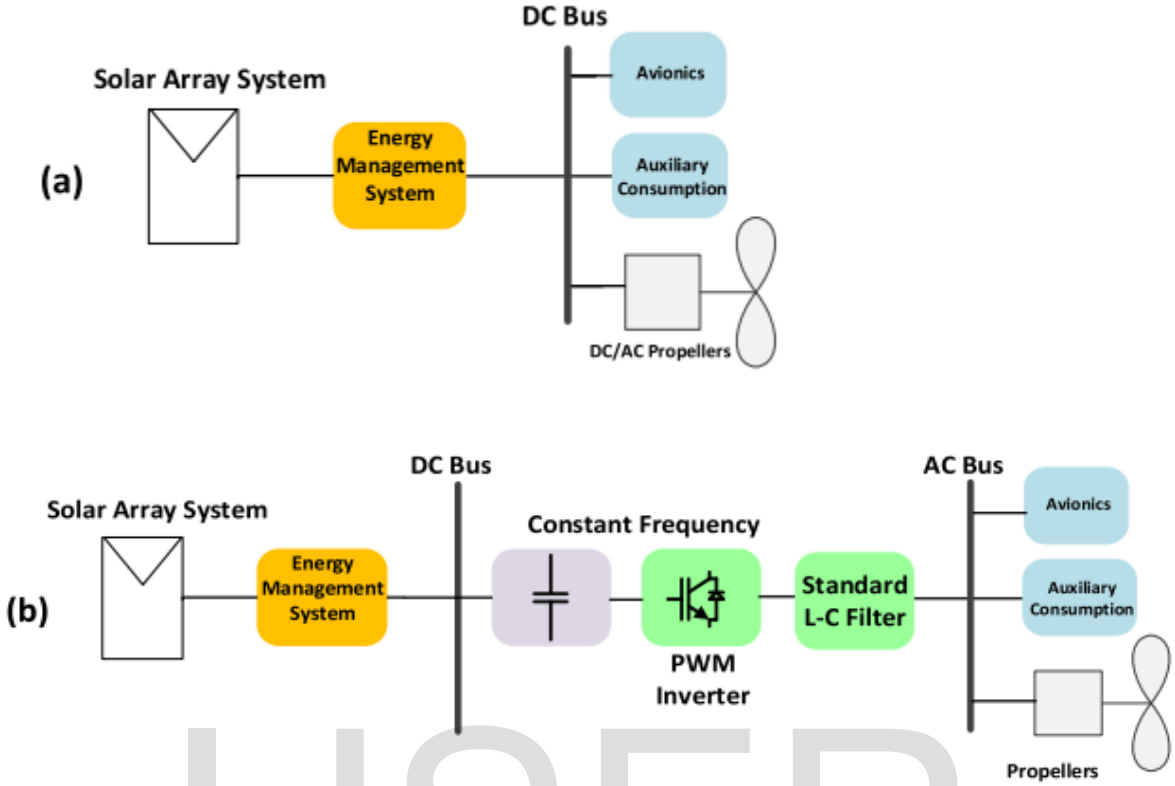

FIGURE 1. Conventional solar powered UAV, (a) Conventional DC bus-line and (b) PWM inverter with standard L-C filter and AC-bus line.

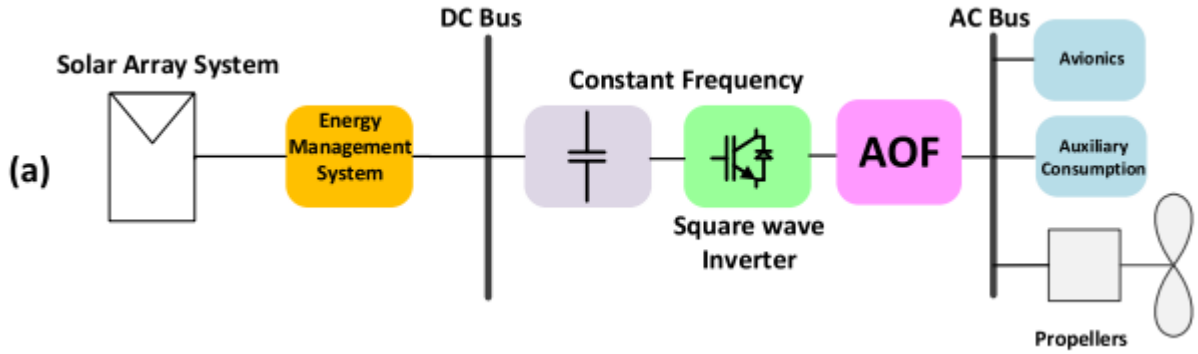

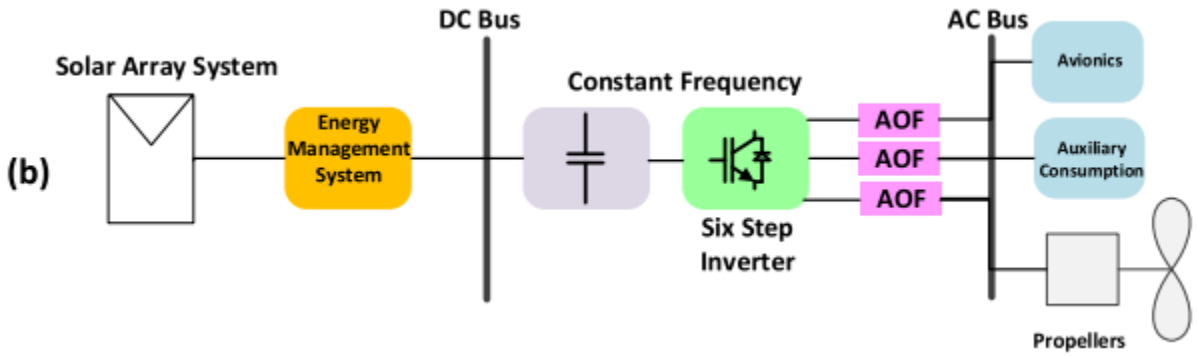

Figure 2. Proposed solar powered UAV and AOF, (a) Single-phase square wave inverter with AC-bus line and (b) Three-phase six-step inverter with AC-bus line.

obtained using the active resistance compensation technique with a total harmonic distortion less than 3%. Moreover, power loss analysis and conversion efficiency calculation of the proposed system are performed and compared with that of the conventional three-phase PWM inverter, where the power loss is improved by 31%. Fig. 2(a) shows the schematic

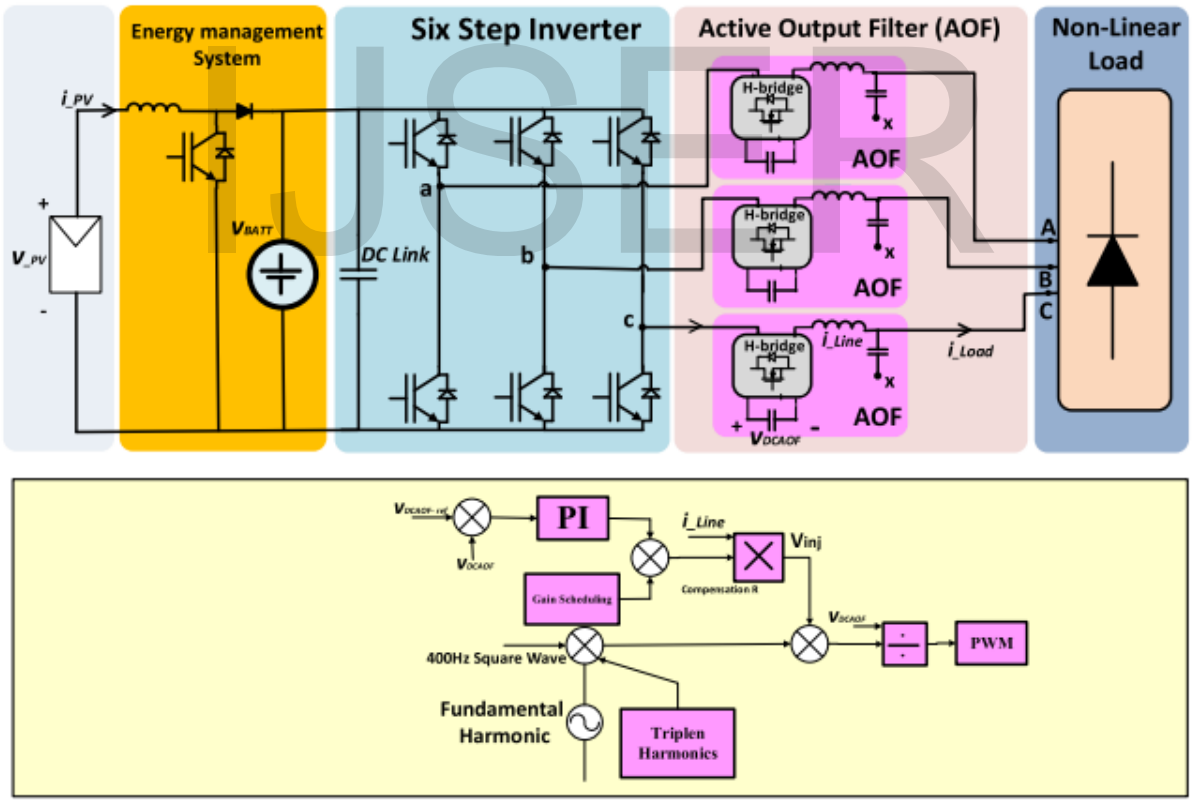

Figure 3. Proposed structure of three-phase electric powertrain for solar powered UAV with AOF integration and its closed-loop control strategy.

diagram of the proposed single-phase square wave inverter with one AOF circuit and AC-bus line, while Fig. 2(b) depicts schematic diagram of the three-phase circuit of the proposed system, which consists of three-phase six-step inverter and three individual AOF H-bridge system with AC-bus line. The proposed systems using 400 HZ switching frequency main inverter and AOF systems are employed in UAV for further reduction in the size of the power transmission system under non-linear load conditions with closed loop control.

PI Controller:

PI controller will eliminate forced oscillations and steady state error resulting in operation of on-off controller and P controller respectively. However, introducing integral mode has a negative effect on speed of the response and overall stability of the system.

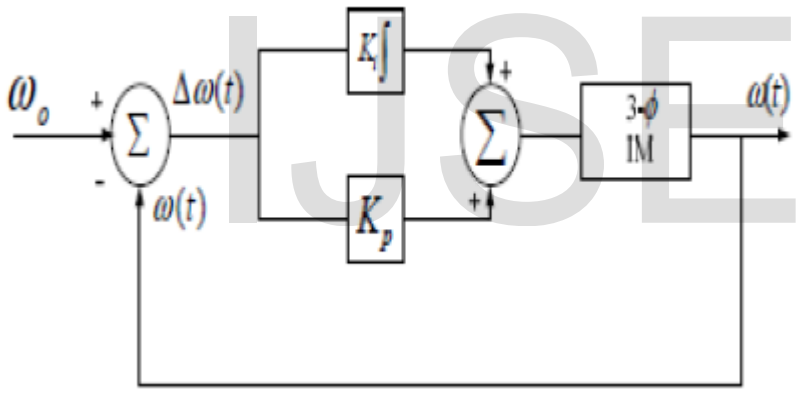

Block diagram of PI controller

The controller output in this case is :u (t) = K p . e(t) + K i∫ e (t) dt

Thus, PI controller will not increase the speed of response. It can be expected since PI controller does not have means to predict what will happen with the error in near future. This problem can be solved by introducing derivative mode which has ability to predict what will happen with the error in near future and thus to decrease a reaction time of the controller.

PI controllers are very often used in industry, especially when speed of the response is not an issue. A control without D mode is used when:

a) Fast response of the system is not required

b) Large disturbances and noise are present during operation of the process

c) There is only one energy storage in process (capacitive or inductive)

d) There are large transport delays in the system

Proposed Solar Powered Unmanned Aerial Vehicle

The structure of the proposed three-phase electric powertrain system of the solar powered UAV with its closed-loop control strategy is illustrated in Fig. 3, which indicates that this structure involves two main parts. The first part is the DC side unit producing DC voltage level, which consists of PV array, DC-DC converter, battery, and power management system. The second part is the AC side unit that consists of three-phase six-step inverter with three-individual AOF of H-bridge topology, which generates sinusoidal AC output voltage for the non-linear load represented by the three-phase diode rectifier. The AOF visualized as a power semiconductor active filter block where the standard LC output filter elements are replaced by a series H-bridge topology. The H-bridge is conducted at a high frequency to introduce voltage harmonics in series with each phase to achieve a sinusoidal output voltage for non-linear loads. The non-linearity of loads results from the recent developments of UAV's loads supplied by rectifier circuits. The proposed power train with AOF has the following advantages: • Low voltage switching for AOFs semiconductor devices. • An extreme decrease in the size of the output LC filter due to high switching frequency operation.

• The use of advanced wide-band gap devices in AOF block design enables high performance while simultaneously reducing the component sizes.

• Produces a high-quality sinusoidal voltage waveforms.

• The use of AOF enables the main inverter to be operated in six-steps or at a reduced PWM switching frequency, thus reducing the conduction power loss, and improving the conversion efficiency.

• AOF is dynamic and can be used for retrofitting applications. In addition, AOF DC-link voltages have the advantage of self-balancing to the third of the DC-link voltage of the main

inverter without the need for close-loop control for linear loads. However, the situation is not similar for highly polluted

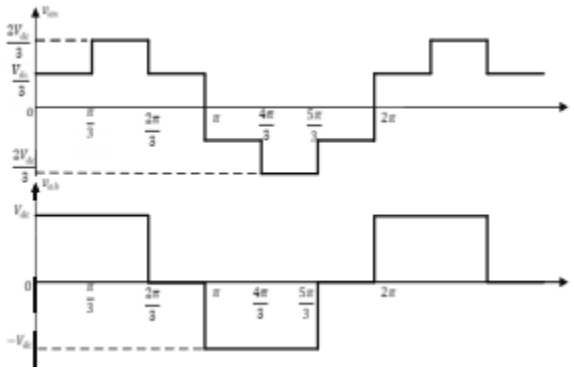

FIGURE 4. Voltage waveforms of six-step inverter.

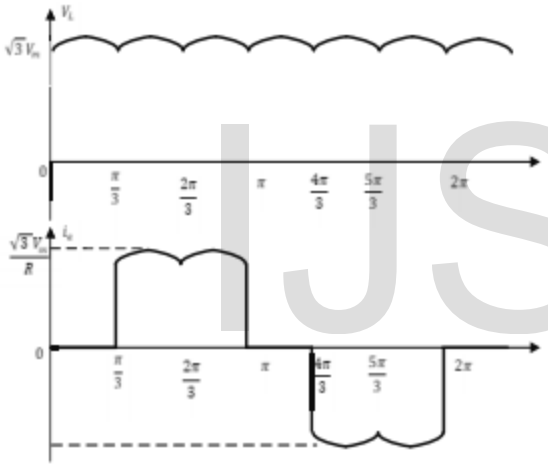

FIGURE 5. Load voltage and line current waveforms of non-linear load.

non-linear loading conditions. Naturally, the non-linear load will advance the current harmonics; These harmonics will be reflected in the AOF DC side. Naturally, the non-linear loads provide current harmonics that will be reflected to AOF DC side, resulting in unbalanced voltage components across the AOF DC link and the line-to-line voltages will be highly distorted. Therefore, AOF topology with open loop control is limited to linear ac loads. In the application of nonlinear loads, The AOF-DC link voltage must be controlled to ensure the voltages across the three DC capacitors is balanced at a value of one-third of the DC bus line voltage of the main inverter. Fig. 3 (b) shows the proposed closed-loop control strategy for AOF to produce an active compensation resistance technique, which is used widely in energy conversion control systems

[30]. The closed-loop control strategy provides a resistance emulator in series with the H-bridge topology which creates a voltage injection across it to dampen the undesirable harmonics generated from the AOF. This active compensation resistances approaches zero at steadystate operation in the case of linear loads [35]. The DC link

voltage of the AOF (Vdc,AOF) is compared to the one-third of the main inverter DC bus-line (Vdc,ref) as shown in Fig. 3(b) and the error signal is provided to a PI and gain scheduling controllers to create the active compensation resistance. The compensation resistance is multiplied by the line current (ia) to produce the injected voltage waveform (vin). The injected voltage contains the reflected harmonics from the non-linear load that need to be included in the main AOF control signal. The actual sensed (Vdc,AOF) voltage is divided by the resulted injected voltage signal obtained previously. Finally, the modeling signal is attained and sent to AOF topology through high switching frequency pulse width modulation technique. III. ANALYSIS AND MODELING The main inverter is a six-step switching inverter that is extensively being used to simplify the control circuit and reduce the switching losses. Low odd harmonics of order n = mp ± 1, where, p is the number of pulses (p = 6) and m being an integer with the absence of triple-n harmonics (n = 3, 6, 9, 15, ...) are generated. The six-step main inverter output line voltage vab and phase voltage van waveforms are shown in Fig. 4, the AC output phase voltages consist of discrete values of voltages, which are Vs 3 , 2Vs 3 , −Vs 3 , −2Vs 3 . The Fourier series expression of the phase voltage van can be given as:

$$v_{an}(t) = \frac{2V_{dc}}{\pi}\left[\sin(\omega t) + \frac{1}{5}\sin(5\omega t) + \frac{1}{7}\sin(5\omega t) + \ldots\right] \quad (1)$$

$$v_{an}(t) = \sum_{k=1,5,7,11\ldots}^{\infty} \frac{2V_{dc}}{\pi k}\sin(k\omega t) \quad (2)$$

nth, with the magnitude of 2Vdc πk , as:

To produce a pure sinusoidal output voltage waveform, the injected voltage of the AOF should be equal in magnitude and opposite in sign to the harmonic contents of the six-step inverter given by Eq. (2). Therefore, the AOF should be controlled to inject the harmonics of orders 5th, 7th, . . . and

$$v_{AOF}(t) = -\sum_{k=5,7,11...}^{\infty} \frac{2V_{dc}}{\pi k} \sin(k\omega t) \qquad (3)$$

The total output voltage across the load terminal is the summation of the inverter output voltage and the AOF produced voltage, and it will be a pure sinusoidal waveform as:

$$v_O(t) = v_{an}(t) + v_{AOF}(t) \qquad (4)$$

$$v_O(t) = \frac{2V_{dc}}{\pi} V_{dc} \sin(\omega t) \qquad (5)$$

Neglecting the ripple at the DC side of the AOF, the switching function SAOF (t) of the AOF can be obtained by dividing the AOF injected voltage with the AOF voltage at the DC side as:

$$S_{AOF}(t) = \frac{v_{AOF}}{V_{dc,AOF}} = -\sum_{k=5,7,11...}^{\infty} \frac{2V_{dc}}{\pi k V_{dc,AOF}} \sin(k\omega t) \quad (6)$$

The AOF dc side voltage Vdc,AOF is controlled at the third of the six-step inverter supply voltage (Vdc 3), and assuming ripple free AOF DC link voltage, the switching function SAOF (t) of the AOF can be simplified as:

$$S_{AOF}(t) = -\sum_{k=5,7,11...}^{\infty} \frac{6}{\pi k} \sin(k\omega t) \qquad (7)$$

The non-linear load is represented by a three-phase bridge rectifier, which is used in medium to high-power application.

It produces a six-pulse ripples on the load voltage waveform having the highest value of the instantaneous line voltage of the supply voltage. The waveforms of the load voltage and ac side line current are shown in Figure 5, where Vm is the maximum phase voltage which is equal to the maximum value of the fundamental component of the six-step inverter 2Vdc π .

The line current shown in Fig. 5 can be described by the Fourier series as

$$i_a(t) = = \frac{2\sqrt{3}V_{dc}}{\pi R}\left[\sin(\omega t) - \frac{1}{5}\sin(5\omega t) - \frac{1}{7}\sin(7\omega t) + \frac{1}{11}\sin(11\omega t) + \frac{1}{13}\sin(13\omega t).....\right] \quad (8)$$

$$i_a(t) = \sum_{k=1,5,7,11...}^{\infty} \pm\frac{2\sqrt{3}V_{dc}}{\pi kR}\sin(k\omega t) \quad (9)$$

The plus or minus sign, symbol ‘‘±,’’ mentions that some terms of the line current harmonics may be added or subtracted depending on its order and the rule can be inferred from the first few terms. The DC link current of the AOF canbe achieved by multiplying the switching function SAOF (t) that controls the AOF and the ac current of ia(t) as:

$$i_{dc,AOF}(t) = S_{AOF}(t).i_a(t) \quad (10)$$

$$= -\sum_{k=5,7,11...}^{\infty}\frac{6}{\pi k}\sin(k\omega t) \times \sum_{n=1,5,7,11...}^{\infty}\pm\frac{2\sqrt{3}V_{dc}}{\pi nR}\sin(n\omega t) \quad (11)$$

$$= -\frac{12\sqrt{3}V_{dc}}{\pi^2 R}\sum_{k=5,7,11...}^{\infty} \times \sum_{n=1,5,7,11...}^{\infty}\pm\frac{1}{nk}\sin(k\omega t) \quad (12)$$

SIMULATION RESULTS

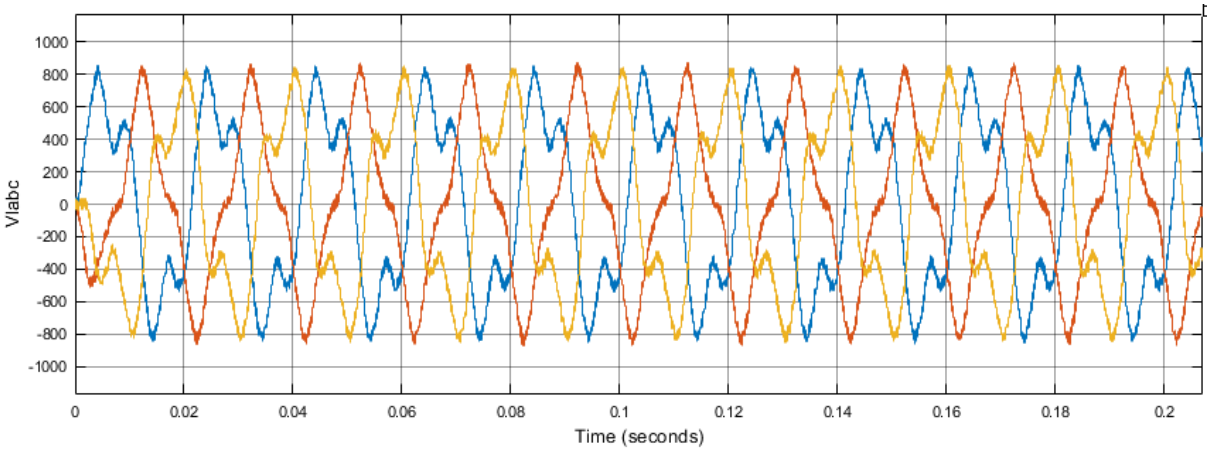

Three-phase line voltages with open-loop control.

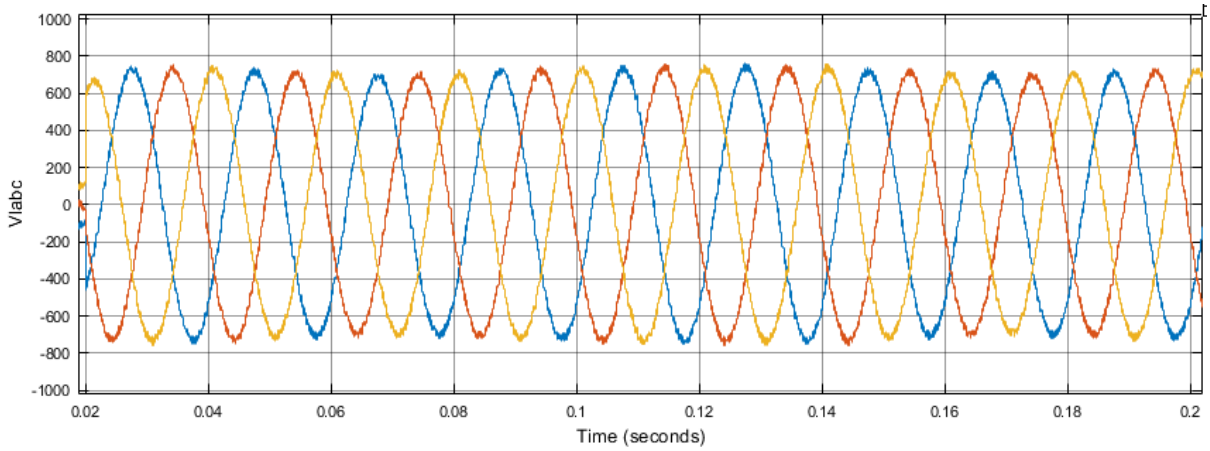

Three-phase line voltages with closed loop control.

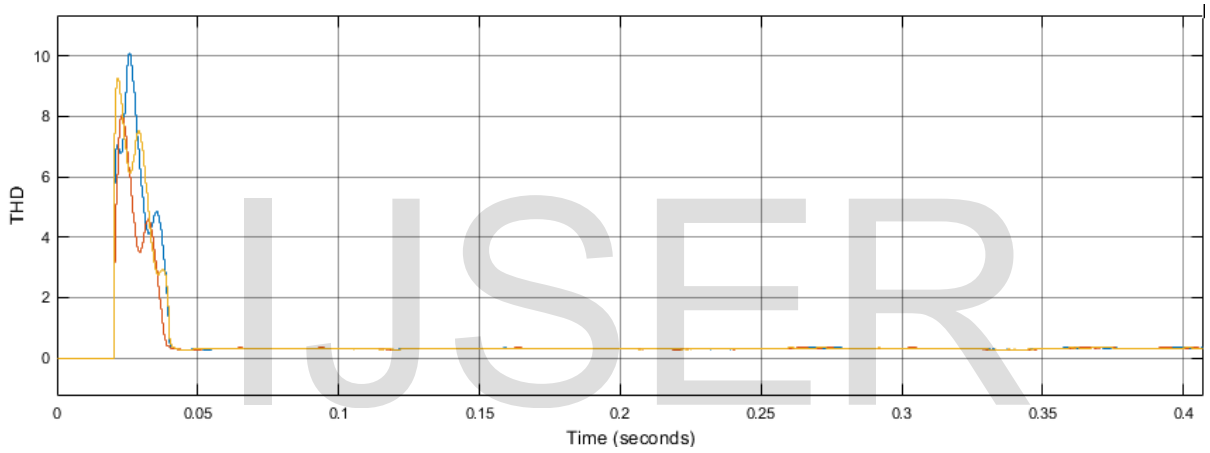

Total harmonic distortion.

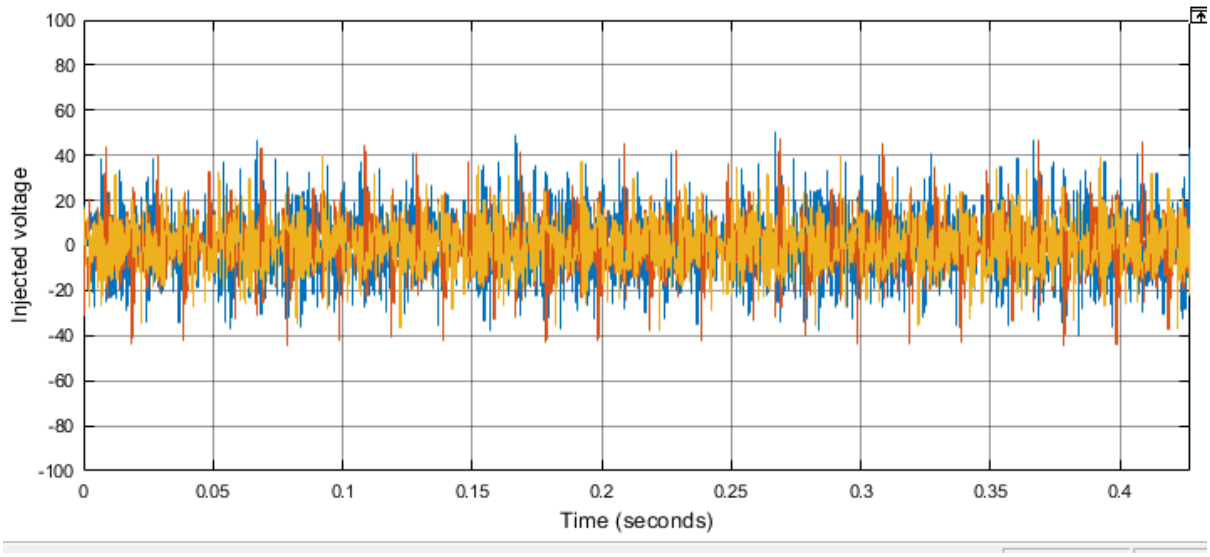

AOF injected voltage

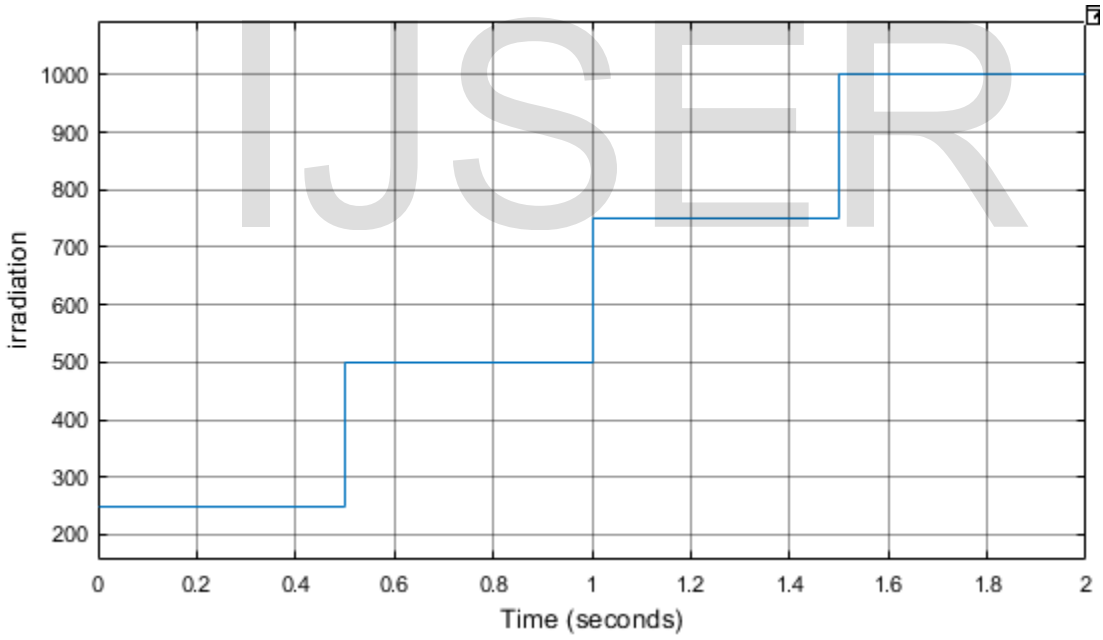

Irradiation

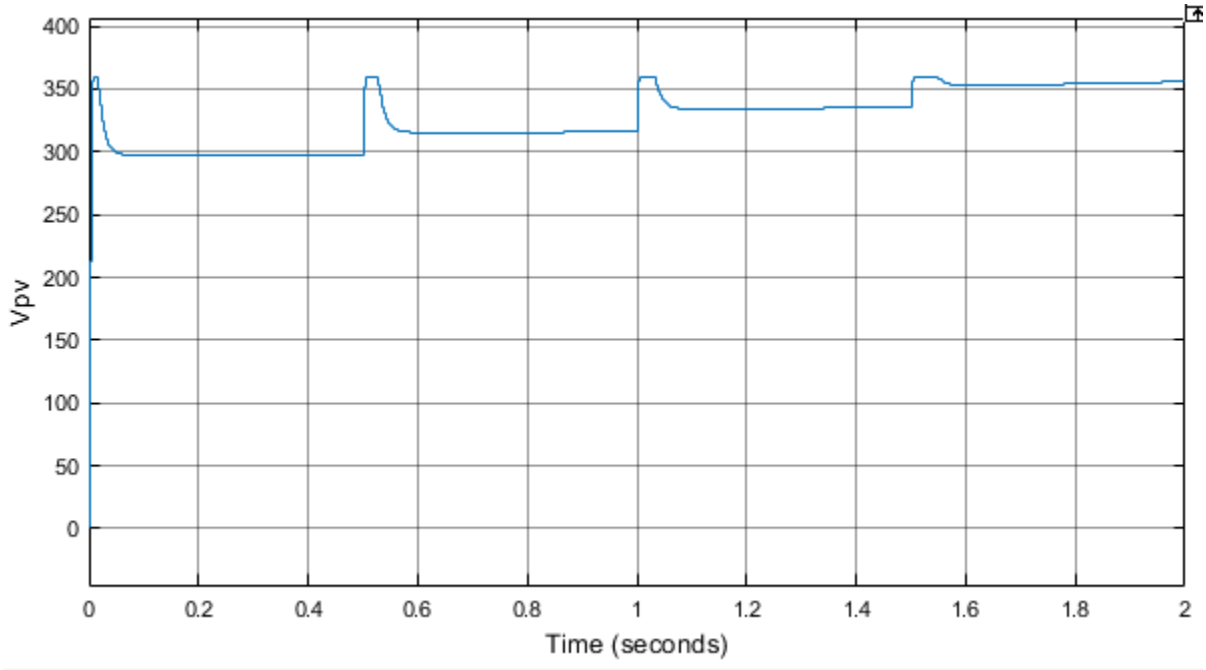

Vpv

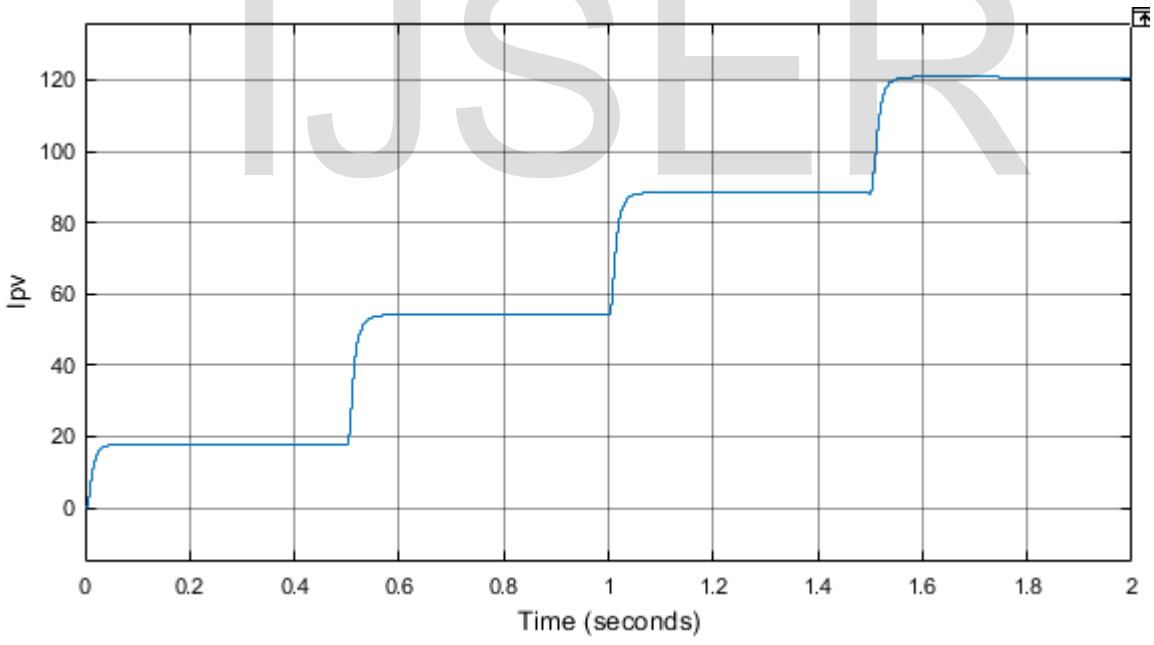

Ipv

CONCLUSION

The obtained simulation results and the voltage and current waveforms demonstrated the viability and the correctness of the proposed power generation system. The proposed active resistance compensation ensures a high-quality sinusoidal line voltage with total harmonic distortion less than 3%. Moreover, power loss analysis and conversion efficiency of the proposed system are performed and compared with that of the conventional three-phase PWM inverter. The obtained results proved that the power loss is reduced by 31%.

REFERENCES [1] U. Burup, P. N. Enjeti, and F. Blaabjerg, ‘‘A new space-vector-based control method for UPS systems powering nonlinear and unbalanced loads,’’ IEEE Trans. Ind. Appl., vol. 37, no. 6, pp. 1864–1870, Nov./Dec. 2001, doi: 10.1109/28.968202. [2] D. Zhang, J. He, and D. Pan, ‘‘A megawatt-scale medium-voltage highefficiency high power density ‘SiC+Si’ hybrid three-level ANPC inverter for aircraft hybrid-electric propulsion systems,’’ IEEE Trans. Ind. Appl., vol. 55, no. 6, pp. 5971–5980, Nov. 2019, doi: 10.1109/TIA.2019.2933513. [3] M. N. Boukoberine, Z. Zhou, and M. Benbouzid, ‘‘A critical review on unmanned aerial vehicles power supply and energy management: Solutions, strategies, and prospects,’’ Appl. Energy, vol. 255, no. 1, pp. 1–22, Dec. 2019, doi: 10.1016/j.apenergy.2019.113823. [4] X. Zhao, J. M. Guerrero, and X. Wu, ‘‘Review of aircraft electric power systems and architectures,’’ in Proc. IEEE Int. Energy Conf. (ENERGYCON), Cavtat, Croatia, May 2014, pp. 949–953, doi: 10.1109/ENERGYCON.2014.6850540. [5] O. D. Dantsker, S. Imtiaz, and M. Caccamo, ‘‘Electric propulsion system optimization for long-endurance and solar-powered unmanned aircraft,’’ in Proc. AIAA Propuls. Energy Forum (EATS), Indianapolis, IN, USA, Aug. 2019, pp. 1–24, doi: 10.2514/6.2019-4486. [6] E. E. Evale, S. Thomas, M. S. Lawal, G. E. Abbe, and E. C. Ashigwuike, ‘‘A novel design technique for electrical power system of ABT-18 unmanned aerial vehicle,’’ in Proc. IEEE 3rd Int. Conf. Electro-Technol. Nat. Develop. (NIGERCON), Owerri, Nigeria, Nov. 2017, pp. 1120–1124, doi: 10.1109/NIGERCON.2017.8281975. [7] B. Luckett, J. He, and R. W. Dyson, ‘‘High-efficiency turboelectric propulsion drive based on medium-voltage SiC indirect matrix converter,’’ in Proc. AIAA Propuls. Energy Forum (EATS), New Orleans, LA, USA, Aug. 2020, pp. 1–7. [8] A. Griffo, R. Wrobel, P. H. Mellor, and J. M. Yon, ‘‘Design and characterization of a three-phase brushless exciter for aircraft starter/generator,’’ IEEE Trans. Ind. Appl., vol. 49, no. 5, pp. 2106–2115, Sep. 2013, doi: 10.1109/TIA.2013.2269036. [9] L. Zhu, D. Jiang, R. Qu, L. M. Tolbert, and Q. Li, ‘‘Design of power hardware-in-the-loop simulations for integrated starter–generator systems,’’ IEEE Trans. Transport. Electrific., vol. 5, no. 1, pp. 80–92, Mar. 2019, doi: 10.1109/TTE.2018.2881052. [10] Z. Hao, X. Wang, and X. Cao, ‘‘Harmonic control for variable-frequency aviation power system based on three-level NPC converter,’’ IEEE Access, vol. 8, pp. 132775–132785, Jun. 2020, doi: 10.1109/ACCESS. 2020.3005192. [11] Z. Zhang, Y. Liu, and J. Li, ‘‘A HESM-based variable frequency AC starter-generator system for aircraft applications,’’ IEEE Trans. Energy Convers., vol. 33, no. 4, pp. 1998–2006, Dec. 2018, doi: 10.1109/TEC. 2018.2867906. [12] A. Eid, H. El-Kishky, M. Abdel-

Salam, and M. T. El-Mohandes, ‘‘On power quality of variable-speed constant-frequency aircraft electric power systems,’’ IEEE Trans. Power Del., vol. 25, no. 1, pp. 55–65, Jan. 2010, doi: 10.1109/TPWRD.2009.2031672.

[13] Z. Zhang, J. Li, Y. Liu, Y. Xu, and Y. Yan, ‘‘Overview and development of variable frequency AC generators for more electric aircraft generation system,’’ Chin. J. Electr. Eng., vol. 3, no. 2, pp. 32–40, Sep. 2017, doi: 10.23919/CJEE.2017.8048410. [14] A. S. Mohamad, ‘‘Modeling of a steady-state VSCF aircraft electrical generator based on a matrix converter with high number of input phases,’’ in Proc. IEEE Student Conf. Res. Develop. (SCOReD), Kuala Lumpur, Malaysia, Dec. 2015, pp. 500–505, doi: 10.1109/SCORED.2015.7449387. [15] V. Biagini, P. Zanchetta, M. Odavic, M. Sumner, and M. Degano, ‘‘Control and modulation of a multilevel active filtering solution for variable-speed constant-frequency more-electric aircraft grids,’’ IEEE Trans. Ind. Informat., vol. 9, no. 2, pp. 600–608, May 2013, doi: 10.1109/ TII.2012.2225433. [16] D. Zhang, J. He, D. Pan, M. Dame, and M. Schutten, ‘‘Development of a high-power density megawatt-scale medium-voltage power converter for aircraft hybrid-electric propulsion systems,’’ in Proc. AIAA/IEEE Electr. Aircr. Technol. Symp. (EATS), Indianapolis, IN, USA, Aug. 2019, pp. 1–6, doi: 10.2514/6.2019-4472. [17] S. Minaei, M. Yildiz, I. C. Göknar, and E. Yuce, ‘‘Negative impedance inverter and all-pass filter realizations using adder and subtractor blocks,’’ in Proc. IEEE 57th Int. Midwest Symp. Circuits Syst. (MWSCAS), College Station, TX, USA, Aug. 2014, pp. 567–570, doi: 10.1109/MWSCAS.2014.6908478. [18] D. Rana, B. Hafez, P. Garg, S. Essakiappan, and P. Enjeti, ‘‘Analysis and design of active inductor as DC-link reactor for lightweight adjustable speed drive systems,’’ in Proc. IEEE Energy Convers. Congr. Expo. (ECCE), Sep. 2014, pp. 3243–3250. [19] E. R. Ribeiro and I. Barbi, ‘‘Harmonic voltage reduction using a series active filter under different load conditions,’’ IEEE Trans. Power Electron., vol. 21, no. 5, pp. 1394–1402, Sep. 2006. [20] J. Chen, X. Zhang, and C. Wen, ‘‘Harmonics attenuation and power factor correction of a more electric aircraft power grid using active power filter,’’ IEEE Trans. Ind. Electron., vol. 63, no. 12, pp. 7310–7319, Dec. 2016. [21] J.-S. Lee and K.-H. Yu, ‘‘Optimal path planning of solar-powered UAV using gravitational potential energy,’’ IEEE Trans. Aerosp. Electron. Syst., vol. 53, no. 3, pp. 1442–1451, Jun. 2017.